

# Unraveling Unidirectional Threading of $\alpha$ -Cyclodextrin in a [2]Rotaxane through Spin Labeling Approach

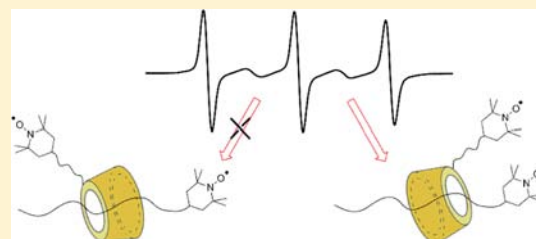
Costanza Casati,<sup>†</sup> Paola Franchi,<sup>†</sup> Roberta Pievo,<sup>‡</sup> Elisabetta Mezzina,<sup>\*,†</sup> and Marco Lucarini<sup>\*,†</sup>

<sup>†</sup>Department of Organic Chemistry "A. Mangini", University of Bologna, Via San Giacomo 11, I-40126 Bologna, Italy

<sup>‡</sup>Max Planck Institute for Biophysical Chemistry am Faßberg 11, 37077 Göttingen, Germany

## Supporting Information

**ABSTRACT:** We present here the results of a CW-ESR investigation of a double spin labeled  $\alpha$ -cyclodextrin-based [2]rotaxane that is characterized by the presence of nitroxide labels both at the wheel and at the dumbbell. This was accomplished by synthesizing a spin labeled  $\alpha$ -CD (the wheel) that was mechanically blocked on a thread containing a nitroxide unit by a Cu(I) catalyzed azide–alkyne cycloaddition (CuAAC). Both ESI-MS analysis and NMR spectroscopy were used to provide evidence of the threading processes. Because of the unsymmetrical structure of both the wheel and the axle, two different geometrical isomers could be predicted on the basis of the orientation of the CD along the thread. By combining molecular dynamic calculations and information extracted from the CW-ESR spectra, we were able to determine the geometrical nature of the isomer that was isolated as the only species. The ESR spectra showed *J*-coupling between the two mechanically connected nitroxide units and were analyzed by a model assuming three main molecular states. The intramolecular noncovalent nature of spin exchange was confirmed by reversibly switching the magnetic interaction on–off by changing the pH of the solution in the presence of a competing macrocyclic host.



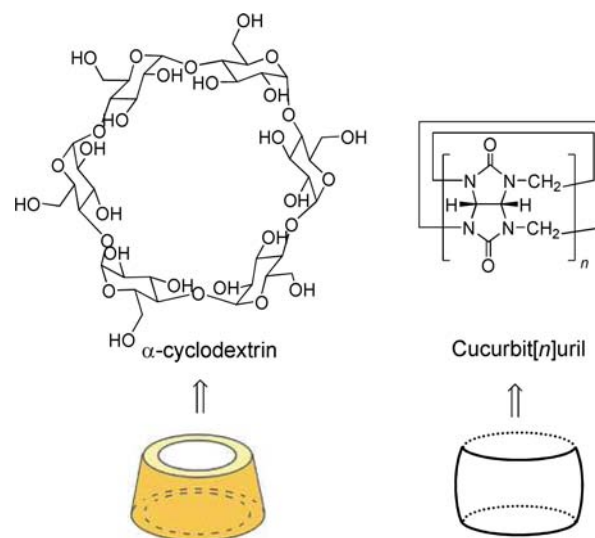
## INTRODUCTION

Cyclodextrins (CDs) continue to be attractive wheel components in constructing mechanically interlocked assemblies, such as rotaxanes.<sup>1,2</sup> A rotaxane is described as a molecular system in which a macrocycle (wheel) threads a linear subunit (dumbbell) with two bulky stoppers. The number of components in a rotaxane is indicated in brackets as a prefix. Therefore, a rotaxane consisting of a single dumbbell and a single macrocycle is indicated as [2]rotaxane.<sup>1,2</sup>

The basis for the construction of a CD-based [2]rotaxane is the interaction between the hydrophobic cavity of the CD and the special hydrophobic unit in the linear component. Since the early 1980s, CD-based [2]rotaxanes have been prepared by encapsulation of a symmetrical linear molecule with CD and subsequent "locking" by coordination or by covalent linking to bulky stoppers.<sup>1,2</sup> At the same time, many unsymmetrical [2]rotaxanes, in which a CD ring encircles an unsymmetrical dumbbell, were also set up.<sup>3–6</sup> In this case, when an asymmetric CD was threaded by a nonsymmetrical dumbbell, it would give two isomers differing in orientation of CD with respect to the different ends of the dumbbell. As a result, two isomeric [2]rotaxanes were always obtained in these systems. The orientations of the CD ring in the isomeric [2]rotaxanes were deduced from NOE measurements or by recording circular dichroism spectra.

It was expected that unidirectional threading of a CD ring by a linear subunit during the formation of a [2]rotaxane could be achieved in order to construct more complicated rotaxanes. However, only in a few cases unidirectional threading of a CD

Chart 1

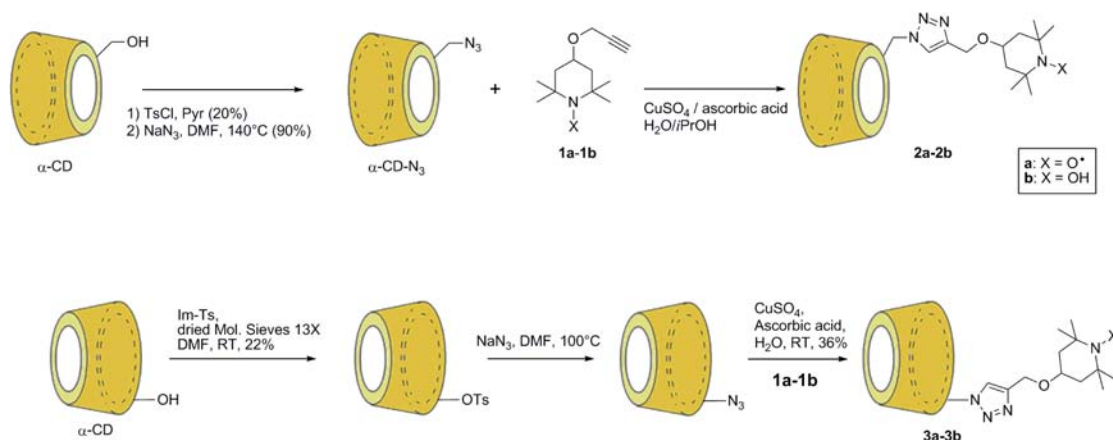


ring by a linear subunit resulting in only one rotaxane isomer was observed.<sup>7,8</sup> In principle, unidirectional threading of a CD ring can be improved by using a functionalized CD at the primary or at the secondary face with appropriate functionalities. Fort and co-workers reported an example of [2]rotaxane

Received: July 26, 2012

Published: October 29, 2012

Scheme 1



having a lactosyl- $\alpha$ -CD conjugate at the primary face and a symmetric decane-based axle carrying lactosyl stoppers at the extremities.<sup>9</sup> Because of the symmetric nature of the axle, however, only one isomer was possible. Thus, the preparation and separation of unidirectional rotaxane in which the CD is monofunctionalized remain totally unexplored.

In past decades, double spin labeling of macromolecules by stable nitroxide radicals has provided remarkable information: in particular, continuous wave (CW) and pulse (e.g., double quantum coherence (DQC) and PELDOR) ESR spectra of double spin labeled systems have been studied.<sup>10,11</sup> The sensitivity of DQC and PELDOR<sup>12,13</sup> spectra allows the reliable determination of distances between labels in the range 1.6–6.0 nm in frozen solution, whereas shorter distances are generally not accessible because the electron dipolar interaction becomes too large and the presence of relevant scalar electron exchange interactions prevents the irradiation of a single electron spin, which is the prerequisite for their application (vide infra).<sup>14</sup>

On the other hand, when the spin labels are at relatively short distances, the liquid solution CW-ESR spectrum could be very informative because its shape depends on several structural and dynamic parameters that characterize the double labeled molecule. Actually, to probe supramolecular complexation by macrocyclic hosts, resorcinarenes,<sup>15</sup> calixarenes,<sup>16</sup> and cyclodextrin<sup>17</sup> containing two nitroxide labels were reported and investigated by CW-ESR.

We have already shown that 2,2,6,6-tetramethylpiperidine-N-oxyl (TEMPO) ring cannot pass through both the cavity of an  $\alpha$ -cyclodextrin<sup>18</sup> and that of cucurbit[6]uril (CB[6]), a synthetic macrocycle largely employed in the preparation of rotaxanes.<sup>19</sup> This feature allowed us to prepare  $\alpha$ -CD- and CB[6]-based rotaxanes having the TEMPO radical as the end-cap group and the above-mentioned macrocycles as the wheel. By using the PELDOR technique, we were able to determine the distances among the paramagnetic end units of the CB[6]-based rotaxane.<sup>20</sup>

As a part of our continuing studies on the characterization of new supramolecular architectures containing open-shell molecules, we present here the results of a CW-ESR investigation of the double spin labeled  $\alpha$ -CD-based [2]rotaxane that is characterized by the presence of two nitroxide free radicals at the wheel and at the dumbbell at several temperatures. In this work we succeed to synthesize for the first time a spin labeled  $\alpha$ -CD (the wheel) and to prepare an unidirectional rotaxane

having a paramagnetic label on the wheel. By combining molecular dynamic calculations and information extracted from the CW-ESR spectra, we were able to determine the geometrical nature of the isolated isomer. Because of great interest in controlling through space spin exchange between two nearby radical centers, we also examined the possibility of reversibly triggering the spin interaction in the reported [2]rotaxane.

## RESULTS AND DISCUSSION

**Synthesis and NMR Characterization of Rotaxanes.** It has already been shown that the TEMPO unit is large enough to be used as the end-cap group in paramagnetic rotaxanes having cucurbit[6]urils<sup>19a</sup> or  $\alpha$ -cyclodextrin<sup>18</sup> as the wheel. While the development of straightforward procedures to functionalize selectively cucurbiturils is still a challenging task,<sup>21</sup> reliable synthetic procedures are available for the functionalization of the primary or the secondary rims of cyclodextrins.<sup>22</sup> For this reason we decided to employ as a paramagnetic wheel an  $\alpha$ -CD functionalized with a nitroxide unit.

Several examples of  $\beta$ -CD containing one or more nitroxide spin labels have been reported in the past.<sup>17,23,24</sup> However, to the best of our knowledge, no paramagnetic  $\alpha$ -CD has been reported in the literature. To this purpose, the new synthesis of two TEMPO-monofunctionalized  $\alpha$ -CDs were undertaken, bringing the radical arm in the larger secondary rim at the 3 position or at the 6 position of the primary rim (Scheme 1).

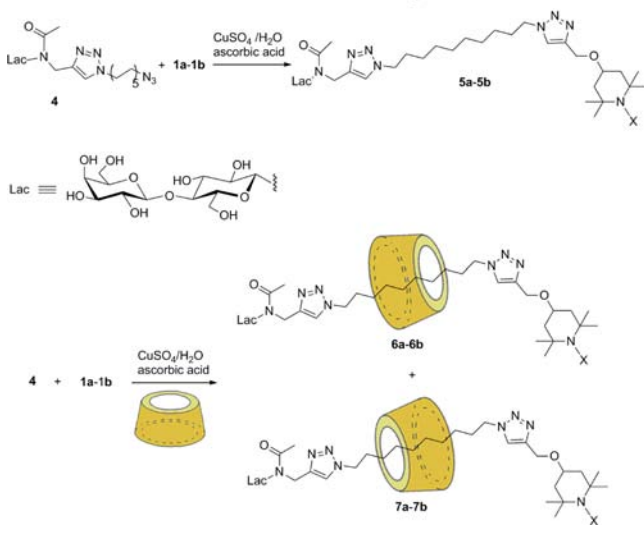
The reactions for the functionalization of the primary rim were realized by selective tosylation of  $\alpha$ -CD,<sup>9,25a</sup> affording pure 6-*O*-Ts- $\alpha$ -CD in 20% yield. The azido derivative<sup>9</sup> was obtained in *N,N*-dimethylformamide (DMF) by tosyl displacement with sodium azide (90% yield). Coupling of the nitroxide alkyne 4-propargyloxy-TEMPO<sup>26</sup> (**1a**, Scheme 1) onto the cyclodextrin, in the presence of a catalytic amount of copper sulfate and sodium ascorbate as reducing agent (*click conditions*), afforded the single 6-triazolyl-TEMPO- $\alpha$ -CD (**2a**) in 48% yield after purification by gel filtration over a Sephadex G-15 column.

The functionalization of the secondary edge of  $\alpha$ -CD was realized according the reaction sequence reported in Scheme 1 starting from  $\alpha$ -cyclodextrin in DMF in the presence of *p*-toluenesulfonylimidazole and freshly activated 4 Å powder molecular sieves, which afforded prevalently mono-2-*p*-toluenesulfonate.<sup>25b</sup> Tosyl displacement with sodium azide<sup>27</sup>

afforded the mono-3-azidodeoxy- $\alpha$ -cyclodextrin.<sup>28</sup> Cu(I) catalyzed 1,3-dipolar cycloaddition of this azide with alkyne **1a** gave **3a** in 36% yield.

In order to prepare the bis-labeled rotaxane, we decided to follow the approach reported by Fort and co-workers<sup>9</sup> based on the formation and assembly by click reaction of a pseudorotaxane composed by  $\alpha$ -CD and a C-10 alkyl chain, blocked at one end by a saccharidic stopper and carrying an azido group at the other end. To check the feasibility of this approach, we initially treated under click conditions the lactosyldecane azide **4** with nitroxide **1a** in the presence of the unmodified  $\alpha$ -CD (Scheme 2). The reaction afforded a

### Scheme 2



mixture of the isomeric rotaxanes **6a** and **7a** (see discussion reported below), differing in the orientation of CDs with respect to the rod's ends, in 22% isolated yield.

Both ESI-MS analysis and NMR spectroscopy were used to provide evidence of the threading processes. In all cases H NMR spectra of the investigated products were recorded after in situ reduction of the sample by Na<sub>2</sub>S<sub>2</sub>O<sub>4</sub> or phenylhydrazine to obtain the corresponding diamagnetic *N*-hydroxy forms (**1b–3b**, **5b–9b**). Although the *N*-hydroxy form of the free thread (**5b**) shows small chemical shift changes in the corresponding H NMR spectra when mechanically trapped inside the macrocycle to form rotaxanes **6b** and **7b**, the 2D ROESY spectrum (Supporting Information) gave clear evidence of the interlocked structure. In particular, we detected strong cross-peaks between the alkyl chain protons of the thread (1–1.4 ppm) and the inner proton of  $\alpha$ -CD, falling in the range 3.7–4.0 ppm. These interactions, which are totally absent in the 2D ROESY spectrum of the free thread **5b**, indicated that the cyclodextrin is located over the rotaxane decamethylene chain, between the lactosyl and TEMPO units.

Because of the unsymmetrical structure of both CD and the axle, a mixture of the two isomers differing in the orientation of CDs with respect to the rod's ends was obtained. The presence of the two isomers with a relative ratio of 70:30 was revealed in the H NMR spectrum of **6b–7b** at 80 °C, by looking at the region around 8 ppm (see Figure 1a). This zone is characterized by the signal due to the aromatic proton of the triazole. The free thread **5b** shows one singlet due to the aromatic proton of triazole next to the nitroxide rod's end and

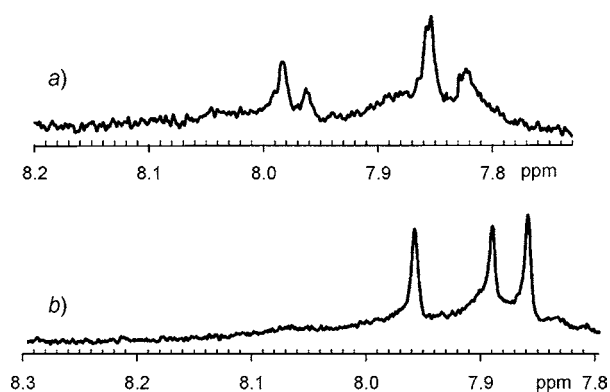


**Figure 1.** <sup>1</sup>H NMR partial spectra (600 MHz, DMSO-*d*<sub>6</sub>, 1.5 mM) of a mixture of rotaxane **6b–7b** (a) and bis-labeled rotaxane (b) showing H triazole signal pattern at 353 K. In the latter case, the presence of three signals corresponding to the different triazole moieties in the molecule is indicative of the formation of only one isomer.

two signals for the proton in the triazole bound to the lactosyl end with the amidic linkage (see Supporting Information). The two signals arise from the restricted rotation of the amidic bond. Actually, tertiary amides are known to undergo a *Z–E* isomerization in solution.<sup>29</sup> At room temperature, two sets of signals corresponding to endo and exo rotamers are commonly observed. Peak coalescence is generally achieved by increasing the temperature, thus making the NMR spectra simpler. Also in our case, at 80 °C, peak coalescence was observed accompanied by a substantial signal broadening for the protons close to the amide group. In the mixture **6b–7b**, all the signals due to the aromatic proton of triazoles are doubled at room temperature, two singlets and two couples of signals that at high temperature coalesce into one, this being an indication of the presence of the two isomeric forms of the rotaxane (see Figure 1a).

The success of the synthesis of this  $\alpha$ -CD-based paramagnetic rotaxane containing lactosyl and TEMPO moieties as stoppers is the basis for the preparation of a new interlocked molecule, in which the bead component consisted of a radical TEMPO- $\alpha$ -CD conjugate. We used both monofunctionalized  $\alpha$ -CDs, bringing the radical arm in the larger secondary rim (**3a**, Scheme 1) and at the 6 position of the primary rim (**2a**, Scheme 1), respectively.

The “click” rotaxation of lactosyl azide **4** with alkyne **1a** in the presence of the monofunctionalized CDs in the condition of the reaction reported in the Scheme 3 provided the desired product only in the case of the 6-armed macrocycle **2a** (vide infra). In the presence of the secondary-armed macrocycle **3a**, no formation of the rotaxane was observed.

The bis-labeled rotaxane was obtained in 29% isolated yield after purification by gel filtration over a Sephadex G-15 column. Its structural determination was provided by ESI-MS and NMR data (Figure 2b). Cross-peaks were detected in the 2D ROESY spectrum involving the alkyl protons of the axle with the inner protons H3 and H5 of  $\alpha$ -CD resonating in the range 3.7–4.0 ppm, which are absent in the free thread.

Because of the unsymmetrical structure of both **2a** and the axle, a mixture of isomers should be predicted on the base of the orientation of the CD along the thread. However, the inspection of the H NMR region around 8 ppm revealed the presence of only one isomer. The *N*-acetate group displays restricted rotation, giving rise to multiplicity of signals in proton NMR spectra. Heating of the material to 60 °C in DMSO shows peak coalescence. At 353 K, the presence of three signals



Scheme 3

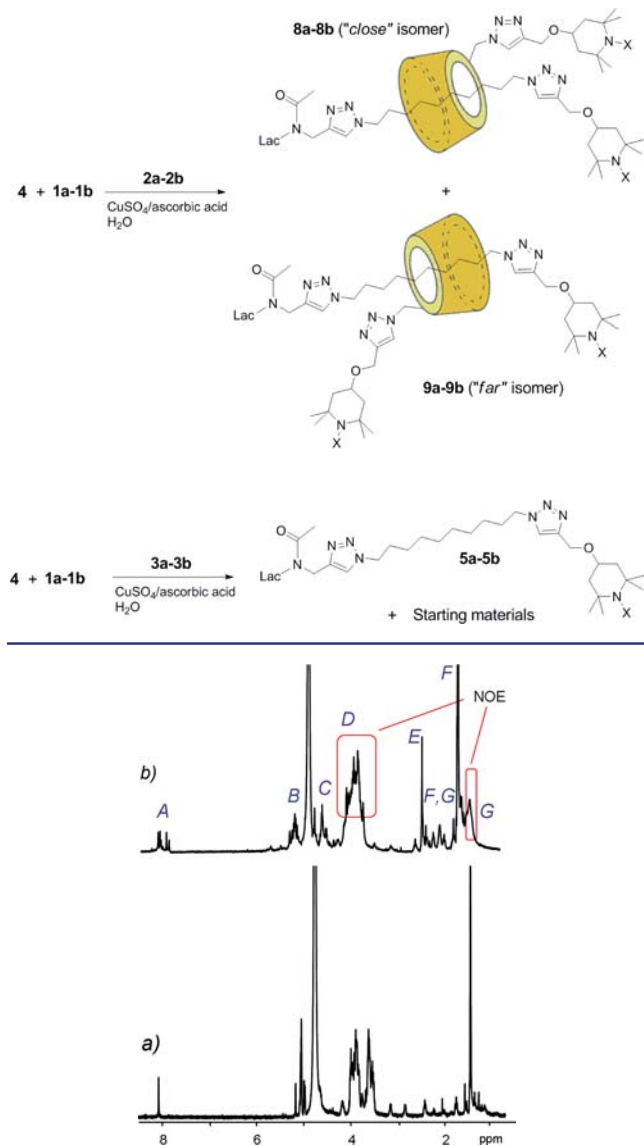


**Figure 2.**  $^1\text{H}$  NMR spectra (600 MHz, 298 K,  $\text{D}_2\text{O}$ , 1.5 mM) of (a) macrocyle **2b** and (b) bis-labeled rotaxane: (A) H triazole; (B) H1 CD,  $\text{CH}_2\text{O TEMPOH}$ , H1 Glu; (C) H1 Gal, N- $\text{CH}_2$ -triazoly,  $\text{CH}_2\text{O TEMPOH}$  and H decane; (D) H-2,3,4,5,6-lactosyl moiety and CD; (E)  $\text{CH}_3$ -CO; (F) TEMPOH; (G) H decane. Signal assignment was achieved by measuring the 2D ROESY spectrum of diamagnetic bis-labeled rotaxane. Square signals give NOE cross-peaks indicating the encapsulation of the decyl thread into the CD.

(Figure 1b) corresponding to the different triazole moieties in the molecule is indicative of the formation of only one species.

It is obvious that the presence of unidirectional bis-labeled [2]rotaxane arises from the formation of only one precursor isomer,  $4@2a$  [2]pseudorotaxane in aqueous media. Such orientation specificity was not observed in the  $4@a$ -CD [2]pseudorotaxane, as two isomeric [2]rotaxanes **6a** and **7a** were obtained in a 70:30 ratio.

The lack of rotaxane formation in the case of the branched CD functionalized in the secondary rim (**3a**) suggests that the substitution of CD in the secondary rim may hamper the inclusion and the threading process of the decamethylene part into the cavity of the host, allowing the inclusion direction of

the azide **4a** to occur only from the secondary edge of CD. If this is true, we can ascribe the unique isolated isomer to the one in which the two spin labels are directed to the same part (**8a**, "close" isomer). However, the NMR data do not permit making any definitive conclusion and CW-EPR spectra were recorded to determine the correct assignment.

**ESR Results.** ESR spectrum of the mixture of monolabeled rotaxanes **6a–7a** (0.05 mM) in water at 328 K is reported in Figure 3a. The expected three-line spectrum is characterized by

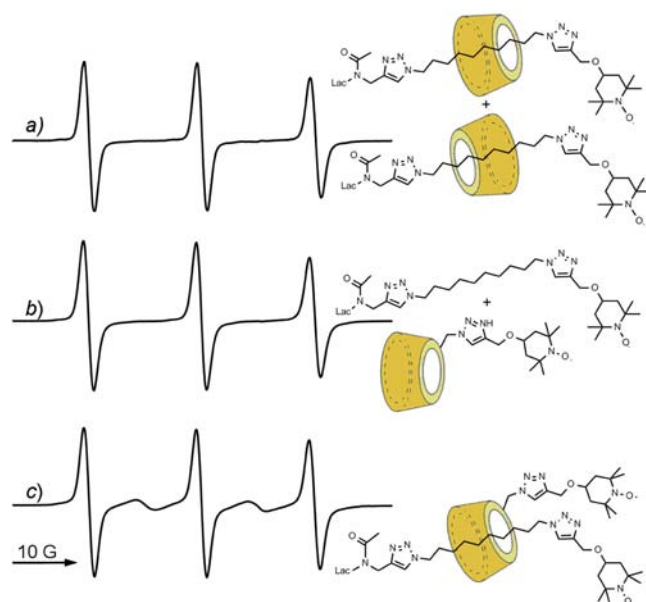


**Figure 3.** ESR spectra of the investigated nitroxides (0.05 mM) recorded in water at 328 K.

the coupling of the unpaired electron with a nitrogen nucleus with a hyperfine splitting constant,  $a_N$ , of 16.97 G ( $g = 2.0056$ ). The high field ESR line is characterized by a lower height with respect to that obtained with free thread, this being due to the slower motion in solution of the rotaxane biradical, resulting in incomplete averaging of the anisotropic components of the hyperfine and  $g$ -tensors. The spectral resolution is not sufficient to allow the detection of the two geometrical isomers, this being an indication that the difference in the  $a_N$  values for the two paramagnetic isomers is smaller than the spectral line width.

ESR spectrum of the bis-labeled rotaxane (0.05 mM) in water at 328 K is reported in Figure 3c.<sup>30</sup> In nitroxide biradicals, the shape of the ESR spectrum is dictated by the degree of  $J$ -coupling between the two electron spins and isotropic hyperfine coupling,  $a_N$ , to the nitroxide nitrogen nucleus.  $J$ -Coupling increases with decreasing distance between labels and therefore reports on the relative interlabel distances.<sup>31–33</sup> When  $J$  is zero, the ESR spectrum is characterized by three hyperfine lines as found for a monoradical nitroxide species. As  $J$  increases, the hyperfine lines broaden and begin to form complex multiplets. When  $J$  becomes large relative to  $a_N$  (strong exchange), the spectrum is characterized by a five-line pattern with an intensity ratio of 1:2:3:2:1 separated by  $a_N/2$ . As observed in Figure 3c, at 328 K, biradical coupling is clearly demonstrated by the presence of five-line pattern, although the second and fourth lines are broader (discussed further below).

Possible mechanisms for  $J$ -coupling can be operative by through-bond or through-space or both. Because of the mechanical linkage between the two nitroxide units, the through bond mechanism can be obviously excluded and the interaction must be related exclusively to through space interaction.

To discard intermolecular  $J$ -coupling between nitroxide labels of two different rotaxane molecules, we recorded under the same condition the ESR spectrum of a mixture containing both the thread, **5a**, and the spin-labeled CD **2a**. As expected, this spectrum is characterized by  $J = 0$  (see Figure 3b).

Because of the through-space nature of  $J$ , we checked by ESR the possibility of reversibly turning on/off the spin interaction by means of an external trigger. This was achieved by simply changing the pH of the solution containing the bis-labeled nitroxide in the presence of anilinium chloride and a macrocyclic host like cucurbit[7]uril (CB[7], Chart 1). Because of the complexation of one or both nitroxide units, addition of CB[7] resulted in the disappearance of the exchange peaks in the ESR spectrum (see Figure 4a). Actually, complexation by

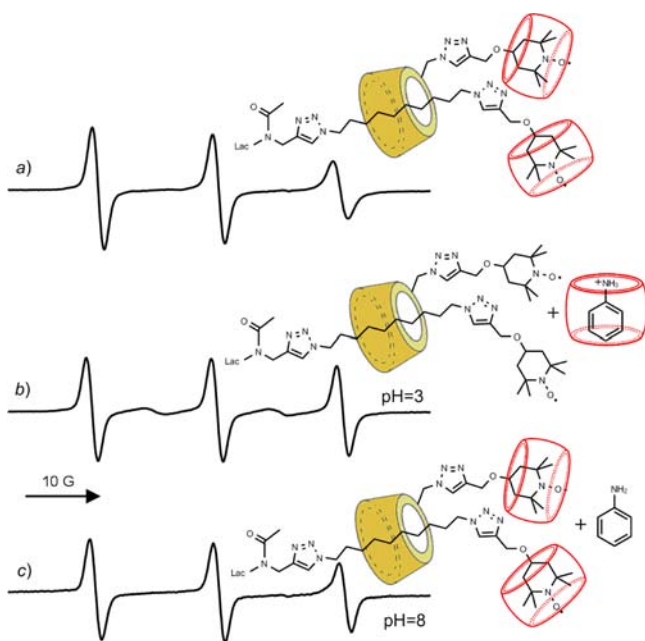


**Figure 4.** EPR spectra of the bis-labeled rotaxane (0.05 mM) in the presence of CB[7] 10 mM: (a) initial solution and in the presence anilinium chloride 25 mM at (b) pH 3 and (c) pH 8.

macrocycles like CD<sup>34</sup> or CB<sup>19a,35</sup> is known to significantly reduce the probability of collisions of the nitroxide termini, giving rise to a complete suppression of spin exchange.

Addition of anilinium chloride (25 mM) at pH 3 (Figure 4b) restored the original five-line pattern, this being an indication that the radicals are completely displaced from the macrocyclic cavity by the aromatic ammonium cation. When increasing the basicity of the solution to pH 8 with NaOH, the second and fourth lines were suppressed again and the monoradical-like spectrum is observed (see Figure 4c). This result strongly suggests that aniline ( $pK_a = 4.6$ ), which is present in alkaline solution, is released from the cavity being replaced by the nitroxide guests. The process is fully reversible: addition of HCl to give back pH 3 results in the formation of a five-line spectrum.

In addition to  $J$ -coupling, nitroxides weakly associated by noncovalent forces can also exhibit electron dipolar coupling.<sup>36</sup> The strength of this interaction is determined by  $1/D^3$ , where  $D$  is the distance between the two nitroxide units. For rapidly tumbling peptides, the dipole–dipole tensor averages to zero and does not contribute to the ESR spectrum. However, for slowly tumbling or immobile systems, the strength of the dipolar interaction serves as a measure of the distance between the coupled spins. At 203 K in water the bis-labeled rotaxane gave the expected spectrum for an immobile nitroxide showing a substantial broadening of the spectral lines as expected for a biradical exhibiting dipolar coupling (see Supporting Information). Because of large distribution of distances, however, a quantitative analysis was not possible.

The ESR spectra of the bis-labeled rotaxane were registered in temperature range 299–360 K (see Figure 5). Considerable

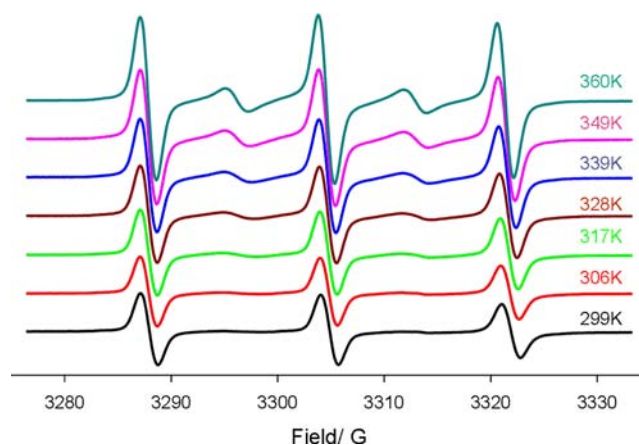


**Figure 5.** ESR spectra of the bis-labeled rotaxane recorded at different temperatures in water.

narrowing of second and fourth lines when the temperature increases indicates unambiguously the fast modulation of the exchange interaction by an intramolecular motion. However, at the temperatures ( $>350$  K) when the widths of second and fourth lines are close to those of outermost lines, the ratio of line intensities differs essentially from 1:2:3:2:1, which is predicted by the model of the diradical with two conformations and with the strong fast exchange ( $J \gg a_N$ ). Thus, the observed distribution of line intensities should be explained by assuming a model with more than two conformations. In this model, proposed by Luckhurst<sup>37</sup> and further developed by Parmon et al.,<sup>38</sup> three main molecular states are considered. In the present case, these states correspond to different coconformations adopted by the  $\alpha$ -CD on the dumbbell component and/or different conformations of the covalent bonds connecting the thread and the spin label. In the first group of conformations (conformation A), the two labels are too far and the radical centers have no opportunity to interact ( $J = 0$ ). In two others (B and C), the TEMPO radical centers get some possibilities to give exchange coupling. In this case, the appearance of the exchange depends on the distance between the radical centers and their mutual orientation. If the average lifetimes of the radical fragments in conformations A,  $\tau_A$ , and in conformations B and C,  $\tau_{B+C}$ , are sufficiently long (i.e.,  $a_N\tau_A > 1$  and  $a_N\tau_{B+C} > 1$ ), a superposition of two ESR spectra will be observed (with statistical weight  $\tau_A/(\tau_A + \tau_{B+C})$  and  $\tau_{B+C}/(\tau_A + \tau_{B+C})$ ). If the movement of the radical fragments in conformations B and C is

fast, the corresponding ESR spectrum will be described by the model of fast exchange.

In the model of three conformations the variation in the width of the second and fourth lines with the temperature can be ascribed to the variation of the modulation conditions for the exchange interaction, while the observed distribution of the line intensities can be explained as a result of the superposition of the ESR spectrum of A and that one due to conformations B and C. The relative intensities of the ESR lines are proportional to the relative lifetimes in the state A and B + C. Thus, theoretical simulation of the experimental spectra afforded the ratio  $I_2/I_1$  between the integrated intensity<sup>39</sup> of the spectral

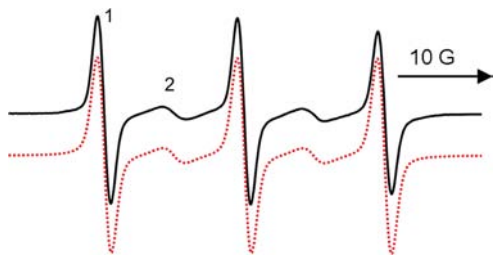


**Figure 6.** ESR spectrum of the bis-labeled rotaxane recorded at 328 K in water (black) and the corresponding theoretical simulation (red).

lines 2 and 1 (see Figure 6) from which the ratio  $\tau_{B+C}/\tau_A$  can be easily calculated by means of the following equation:

$$\frac{\tau_{B+C}}{\tau_A} = \frac{3(I_2/I_1)}{2 - (I_2/I_1)} \quad (1)$$

As an example, in Figure 6 is reported the excellent agreement between the experimental ESR spectrum of the bis-labeled rotaxane recorded at 328 K and the corresponding theoretical simulation obtained by using the three conformations model and  $\tau_{B+C}/\tau_A = 0.76$ .

The  $\tau_{B+C}/\tau_A$  ratio increases as the temperature rises. This dependence can be approximated by a straight line (Figure 7) according to eq 2:<sup>38,40</sup>

$$\ln \frac{\tau_{B+C}}{\tau_A} = \frac{\Delta S}{R} - \frac{\Delta H}{RT} \quad (2)$$

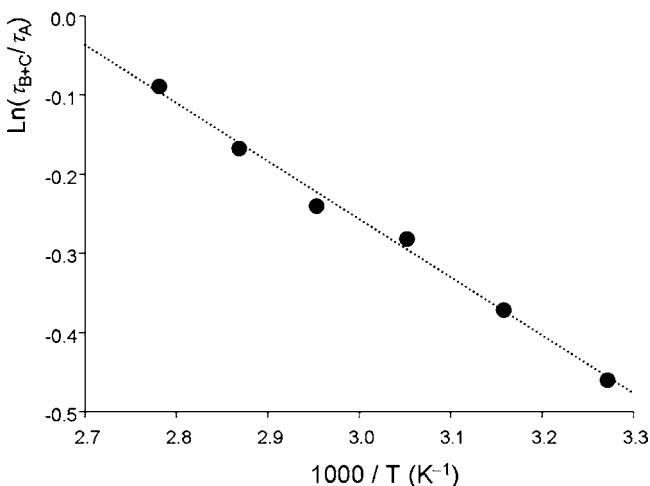


**Figure 7.** Lifetime  $\tau_{B+C}/\tau_A$  ratio as a function of temperature.

Analysis of the dependence of  $\tau_{B+C}/\tau_A$  on temperature afforded changes of entropy and enthalpy for the equilibrium as  $\Delta H = +1.45 \text{ kcal mol}^{-1}$  and  $\Delta S = +3.85 \text{ cal mol}^{-1} \text{ K}^{-1}$ .

We can tentatively assign the three different ESR species to three different groups of the mechanically interlocked biradicals. The temperature dependence of  $\tau_{B+C}/\tau_A$  indicates that A is the more stable group of conformations. In these conformations the radical centers are not able to interact and  $J = 0$  (Scheme 4A). Any displacement of the macrocycle from this equilibrium position results in a new group of conformations where the TEMPO radical centers get some possibilities to give exchange coupling. We attributed these displacements to movements of the macrocycle along and/or around the thread which are expected to be slow in the ESR time scale as indicated by the superposition of the ESR signals due to group conformations A and B + C. This is in line with previous reports showing that threading of paramagnetic guest molecules in the cyclodextrin cavity is generally slow in the ESR time scale.<sup>41</sup> The small enthalpy and entropy variations observed for the transition between A and B + C conformations suggest that the interaction of  $\alpha$ -CD with the thread is very similar in the two group of conformations. This is in agreement with a theoretical investigation performed on cyclodextrin-based rotaxanes showing that the interaction between  $\alpha$ -CD and an aliphatic thread does not change significantly by varying the position of the macrocycle on the linear chain.<sup>42</sup>

On the other hand, the exchange between conformations B and C is fast in the ESR time scale as indicated by the time-dependent modulation of  $J$ -coupling. We attributed this exchange to conformational freedom about both the two chains bearing the spin labels (Scheme 4B,C).

**Molecular Dynamics.** The main question about the nature of the geometrical isomer remains open. This problem can be translated into a question of distance distribution of the two labels that are attached to the thread and the macrocycle. This distance is determined both by coconformation adopted by the  $\alpha$ -CD on the paramagnetic dumbbell component and by the conformation adopted by the covalent bonds on the chain and on the label. Thus, stochastic dynamics (SD) simulations were performed in water at 328 K on the two possible isomers 8a and 9a by using the AMBER\* force field (see Figure 8). The N–O bond was modeled by the C=O bond owing to their similar geometries and the higher reliability of the parameters of the latter group in the AMBER\* force field.<sup>43</sup>

A Monte Carlo conformational search was carried out by rotating all C(sp<sup>3</sup>)–C(sp<sup>3</sup>), Ar–C(sp<sup>3</sup>), O–C(sp<sup>3</sup>), and N–C(sp<sup>3</sup>) bonds in the thread and in the CD radical arm. The most stable conformation found by this procedure was that one used in the dynamic simulation.

The computational approach taken in this study is to dock the thread inside the host cavity, energy-minimize the mechanical complex, and carry out standard equilibrations and production runs to derive distance distributions,  $p(r)$ , between the midpoint of N–O• bonds. To accomplish this, we began with a substituted cyclodextrin having a 6-fold symmetric cavity with the thread docked in its interior. We selected a symmetric CD cavity only as a guide for the placement of the guest and with the awareness that the presence of the paramagnetic arm will result in a deformation of the macrocycle cavity upon geometry optimization. The origin of a Cartesian reference frame was placed at the center of mass of the CD with the  $z$  axis aligned with the C6 symmetry axis of CD. A second reference frame was placed on the thread molecule with the  $z$



## Scheme 4. Possible Conformations of the Bis-Labeled Rotaxane

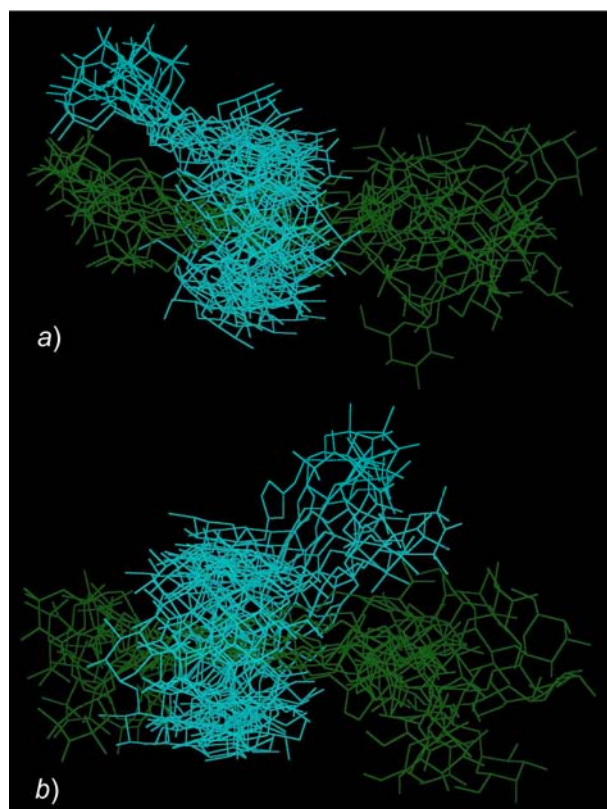
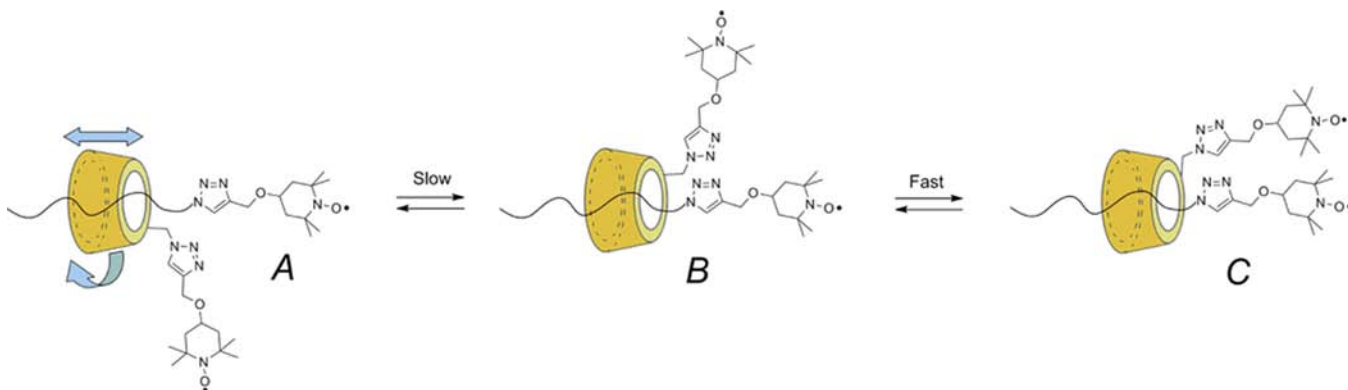


**Figure 8.** Clustered molecular display. Molecular dynamics of the bis-labeled rotaxanes **8a** (a) and **9a** (b). Drawings include 20 structures that refer to the 50 ns simulation. Hydrogens have been omitted for clarity.

axis passing through the C(5)–C(6) bond of the alkyl chain. The thread was translated along the  $z$  axis in order to have the C(6) located in the plane passing through the six acetal oxygens of the CD. At the end of this procedure, minimization of the rotaxane led to the starting geometry for stochastic dynamics (SD) simulations. The simulations were run at 328 K for 50 ns with time steps of 1 fs and an equilibrium time of 5 ns before each dynamic run.

In Figure 9, estimates of  $p(r)$  from MD calculations are reported. As expected for the two isomers, very different distance profiles were obtained with  $\langle p(r) \rangle$  corresponding to 11.35 Å and 21.96 Å for the “close” (blue) and “far” (red) isomers, respectively. It is important to note that the occurrence of distances smaller than 15 Å in the “far” isomer

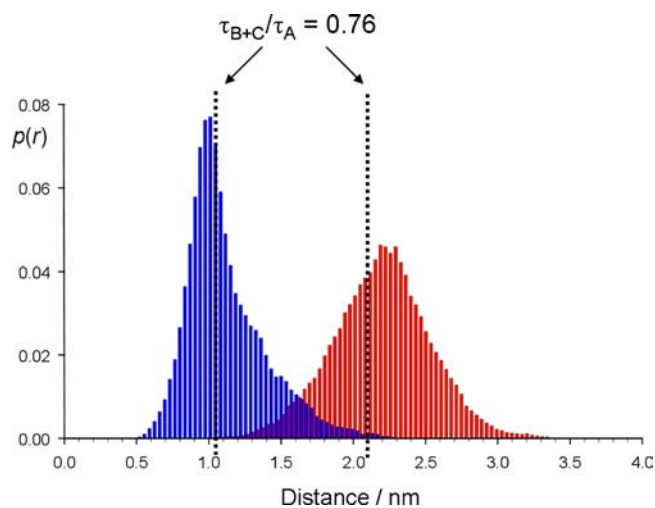
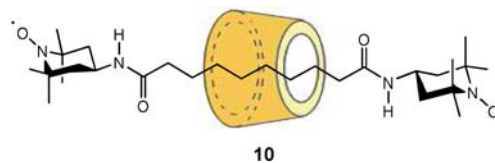


**Figure 9.** Distance distributions,  $p(r)$ , between the midpoint of N–O• bonds determined by MD simulations at 328 K in water for carbonyl analogues of **8a** (“close” isomer, blue) and **9a** (“far” isomer, red).

is negligible. Some years ago we reported the CW-ESR spectrum of a paramagnetic rotaxane (**10**) having an octamethylene chain flanked by TEMPO groups as the thread and  $\alpha$ -CD as the wheel (Scheme 5).<sup>18</sup>

## Scheme 5



This ESR spectrum recorded in water consists of *only three lines*, indicating that the biradical thread is constricted in an extended conformation in which the TEMPO fragments behave as two single nitroxide radicals and  $J = 0$ . We repeated MD simulation also for this structure (see Supporting Information), and we obtained rather narrow distance distributions,  $p(r)$ , in which all distances are larger than 15 Å. This result clearly led to the conclusion that the presence of exchange peaks in the ESR spectrum of the bis-labeled rotaxane (Figure 3c) is not compatible with the  $p(r)$  profile found by MD for the “far” isomer.

Further evidence to this hypothesis was obtained by performing PELDOR<sup>44–47</sup> measurements on rotaxane **8a**. The X-band PELDOR time traces of the bis-labeled rotaxane were performed in H<sub>2</sub>O at 40 K and did not display any pronounced dipolar oscillation (see Supporting Information). Attempts to deduce a distance distribution profile from the analysis of the data were unsuccessful, this being an indication of the absence of spin pairs with distances of  $\geq 15$  Å.

Many experimental and theoretical studies have been devoted to the dependence of the exchange coupling upon structural parameters.<sup>31,32</sup> Nevertheless, the dependence of the electron spin–spin exchange interaction between unpaired electrons ( $J$ ) on three-dimensional structural parameters remains challenging because the modulation of the exchange interaction, due to the large conformational freedom of the investigated systems, limits the utility of their applications. It has been shown that the exchange coupling constant  $J$  decreases exponentially with the distance<sup>48</sup> and that it depends on the orientation of the orbitals containing the unpaired electron with respect to each other.<sup>49</sup> It is also generally accepted that  $J$  is negligible when two N–O bonds are separated by a distance larger than 8–9 Å and interact only through space.<sup>48b,50</sup>

By combination of our ESR and MD results, it is possible to support the last supposition. Simulation of the ESR spectrum of **8a** recorded at 328 K afforded a ratio  $\tau_{B+C}/\tau_A = 0.76$  (see Figure 6). This ratio corresponds to a 57% of structures in which  $J$  is 0. In the  $p(r)$  profile obtained by MD calculations, this corresponds to distances larger than 10.1 Å for the “close” isomer and 21.0 Å for the “far” isomer (see Figure 9). While the above distance limit is unrealistic for the “far” isomer, the value found with the “close” isomer is in excellent agreement with the hypothesis considering  $J = 0$  when distances are larger than 8–9 Å.<sup>51</sup>

On the basis of the above consideration we can definitively conclude that the rotaxane was isolated in the **8a** isomer form (“close” isomer).

## CONCLUSIONS

We reported the synthetic procedure for the preparation of a bis-nitroxide rotaxane by click chemistry. The findings presented here demonstrate that ESR of doubly TEMPO labeled rotaxanes is a useful technique to unravel unidirectional threading of  $\alpha$ -cyclodextrin in a [2]rotaxane and to study quantitatively the dynamics of intramolecular collisions of the molecular fragments mechanically connected. While it is reassuring that crystallography and solution magnetic resonance are primary techniques to characterize mechanically interlocked molecules, it is also clear that important new information is available from solution studies of spin-labeled rotaxanes by ESR.

## EXPERIMENTAL SECTION

ESR spectra has been recorded by using the following instrument settings: microwave power 0.79 mW, modulation amplitude 0.04 mT, modulation frequency 100 kHz, scan time 180 s, 2K data points.

PELDOR experiments at 40 K of the bis-labeled rotaxane (100  $\mu$ M in H<sub>2</sub>O, 10% glycerol) were performed using a Bruker ELEXSYS E-580 X/Q-band spectrometer equipped with a ER4118X-MDS-W1 resonator at the X band (microwave frequency 9.4 GHz) (see also Supporting Information).

<sup>1</sup>H and 2D NMR spectra were recorded at 298 K on a Varian Inova spectrometer operating at 600 MHz in D<sub>2</sub>O solutions using the solvent peak as an internal standard (4.76 ppm). <sup>13</sup>C NMR spectra

were recorded on a Varian Inova operating at 125 MHz in D<sub>2</sub>O solutions using DSS (3-(trimethylsilyl)-1-propanesulfonic acid, sodium salt) as an external standard. Chemical shifts are reported in parts per million ( $\delta$  scale). ROESY data were collected using a 90° pulse width of 6.7  $\mu$ s and a spectral width of 6000 Hz in each dimension, respectively. The data were recorded in the phase sensitive mode using a CW spin-lock field of 2 kHz, without spinning the sample. Acquisitions were recorded at mixing times of 300 ms. Other instrumental settings were 64 increments of 2K data points, 8 scans per  $t_1$ , 1.5 s delay time for each scan.

ESI-MS spectra were recorded with Micromass ZMD spectrometer by using the following instrumental settings: positive ions; desolvation gas (N<sub>2</sub>), 230 L/h; cone gas (skimmer), 50 L/h; desolvation temp, 120 °C; capillary voltage, 3.2 kV; cone voltage, 40 and 100 V; hexapole extractor, 3 V.

All reagents were commercially available and were used without further purification. Compounds **4**,<sup>9</sup> **1**,<sup>26</sup> 6-*O*-*p*-toluenesulfonyl- $\alpha$ -cyclodextrin,<sup>9,25a</sup> 6-azido-6-deoxy- $\alpha$ -cyclodextrin,<sup>6</sup> 2-*O*-*p*-toluenesulfonyl- $\alpha$ -cyclodextrin,<sup>25b</sup> and 3-azido-deoxy- $\alpha$ -cyclodextrin<sup>27</sup> were synthesized according to literature procedure.

**Compound 2a.** Ascorbic acid (0.032 g, 0.18 mmol) and copper sulfate (0.017 g, 0.07 mmol) were added to a solution of 6-azido-6-deoxy- $\alpha$ -cyclodextrin (0.35 g, 0.35 mmol) and **1a** (0.074 g, 0.35 mmol) in 2:1 H<sub>2</sub>O/*i*-PrOH (10 mL). The reaction mixture was stirred for 72 h at room temperature and evaporated under reduced pressure. The crude residue was purified by column chromatography (silica gel, eluent CH<sub>3</sub>CN/H<sub>2</sub>O, 85:15) and gel exclusion over Sephadex column G15 (0.2 g, 48.5%).  $\delta_H$  2.80–2.90 (m, 1 H), 3.15–3.25 (m, 1 H), 3.50–4.10 (m, 34 H), 4.19 (m, 1 H), 4.60–4.70 (m, 2 H), 4.95–5.19 (m, 8 H), 8.00–8.10 (bs, 1 H). ESI-MS  $m/z$  1208.3 [M + H]<sup>+</sup>, 1230.3 [M + Na]<sup>+</sup>. The <sup>1</sup>H NMR spectrum of **2b** was measured after Na<sub>2</sub>S<sub>2</sub>O<sub>4</sub> in situ reduction of the sample containing the nitroxide **2a**.  $\delta_H$  1.46 (s, 12 H), 1.76 (t,  $J = 12$  Hz, 2 H), 2.42 (t,  $J = 12$  Hz, 2 H), 2.86 (d,  $J = 12$  Hz, 1 H), 3.15 (d,  $J = 12$  Hz, 1 H), 3.50–4.10 (m, 32 H), 4.19 (m, 1 H), 4.60–4.70 (m, 2 H), 4.96 (s, 1 H), 4.99 (d,  $J = 2.4$  Hz, 1 H), 5.03–5.10 (m, 5 H), 5.16 (s,  $J = 1.8$  Hz, 1 H), 8.07 (s, 1 H).

**Compound 3a.** Ascorbic acid (0.023 g, 0.13 mmol) and copper sulfate (0.032 g, 0.13 mmol) were added to a solution of 3-azidodeoxy- $\alpha$ -cyclodextrin (0.13 g, 0.13 mmol) and **1a** (0.027 g, 0.13 mmol) in H<sub>2</sub>O (5 mL). The reaction mixture was stirred at room temperature overnight and evaporated under reduced pressure. The crude residue was purified by gel exclusion over Sephadex column G15 (0.1 g, 63.8%).  $\delta_H$  3.50–4.15 (m, 34 H), 4.46 (m, 2 H), 5.00–5.20 (m, 6 H), 8.30–8.40 (bs). ESI-MS  $m/z$  1208.3 [M + H]<sup>+</sup>, 1230.3 [M + Na]<sup>+</sup>. The <sup>1</sup>H NMR spectrum of **3b** was measured after Na<sub>2</sub>S<sub>2</sub>O<sub>4</sub> in situ reduction of the sample containing the nitroxide **3a**.  $\delta_H$  1.44 (s, 12 H), 1.75 (m, 2 H), 2.37 (m, 2 H), 3.50–4.10 (m, 35 H), 4.13 (m, 1 H), 4.46 (m, 2 H), 5.02–5.16 (m, 6 H), 8.34 (s, 1 H).

**Rotaxanes 6a/7a.** To an aqueous solution (5 mL) of  $\alpha$ -CD (0.06 g, 0.062 mmol) and lactosyl azide (**4**) (0.04 g, 0.062 mmol) stirred for 15 min, alkyne **1a** (0.015 g, 0.073 mmol), ascorbic acid (0.005 g, 0.025 mmol), and copper sulfate (0.003 g, 0.012 mmol) were added. The mixture was stirred for 72 h at room temperature. After evaporation under reduced pressure the crude was purified by column chromatography (silica gel, eluent CH<sub>3</sub>CN/H<sub>2</sub>O, 9:1, to CH<sub>3</sub>CN/H<sub>2</sub>O/30% NH<sub>3</sub>, 8:2:1) and gel exclusion over Sephadex column G15 (0.024 g, 22%).  $\delta_H$  1.00–1.55 (m, 12 H), 1.58–1.66 (m, 2 H) 1.72–1.90 (m, 4 H), 1.94–2.04 (m, 2 H), 2.20–2.28 (m, 3 H), 3.50–4.00 (m, 47 H), 4.32–4.54 (m, 7 H), 4.60–4.66 (m, 2 H), 5.04–5.15 (m, 7 H), 7.90–8.10 (m, 2 H). ESI-MS  $m/z$  1851.6 [M + Na]<sup>+</sup>. The <sup>1</sup>H NMR spectrum of **6b/7b** was measured after Na<sub>2</sub>S<sub>2</sub>O<sub>4</sub> in situ reduction of the sample containing the nitroxides **6a/7a**.  $\delta_H$  1.00–1.40 (m, 12 H), 1.44 (brs, 12 H), 1.50–1.65 (m, 2 H), 1.75–1.85 (m, 4 H), 1.94–2.04 (m, 2 H), 2.20–2.26 (m, 3 H), 3.50–4.00 (m, 47 H), 4.15 (m, 1 H), 4.34–4.54 (m, 7 H), 4.62–4.66 (m, 2 H), 5.04–5.15 (m, 7 H), 7.86–8.09 (m, 2 H).

**Compound 5a.** This product was obtained as byproduct by purification of rotaxane **6a/7a** or **8a**.  $\delta_H$  1.00–1.25 (m, 12 H), 1.80–1.92 (m, 4 H), 2.23 (brs, 3 H), 3.52–4.10 (m, 12 H), 4.30–4.60 (m, 7 H), 5.10–5.18 (m, 0.75 H), 5.60–5.64 (m, 0.25 H), 7.87–8.16 (m, 2



H). ESI-MS  $m/z$  878.67  $[M + Na]^+$ . The  $^1H$  NMR spectrum of **5b** was measured after  $Na_2S_2O_4$  in situ reduction of the sample containing the nitroxide **5a**.  $\delta_H$  1.12–1.28 (m, 12 H), 1.30–1.42 (m, 12 H), 1.50–1.74 (m, 2 H), 1.80–1.95 (m, 4 H), 2.10–2.26 (m, 5 H), 3.55–4.05 (m, 14 H), 4.30–4.70 (m, 7 H), 5.12 (d,  $J = 7.8$  Hz, 0.75 H), 5.61 (d,  $J = 9.6$  Hz, 0.25 H), 7.88 (s, 1 H), 8.01 (s, 0.25 H), and 8.05 (s, 0.75 H).

**Rotaxane 8a**. To an aqueous (3 mL) solution of **2a** (0.05 g, 0.041 mmol) and **4** (0.026 g, 0.041 mmol) stirred for 15 min, alkyne **1a** (0.01 g, 0.05 mmol), ascorbic acid (0.003 g, 0.016 mmol), and copper sulfate (0.002 g, 0.008 mmol) were added. The mixture was stirred for 72 h at room temperature. After evaporation under reduced pressure the crude was purified twice by gel exclusion over Sephadex column G15 (0.025 g, 29%).  $\delta_H$  1.08–1.44 (m, 12 H), 1.80–1.90 (m, 4 H), 1.93–2.03 (m, 2 H), 2.23 (m, 3 H), 2.80–3.04 (m, 1 H), 3.50–4.20 (m, 45 H), 4.32–4.54 (m, 8 H), 4.58–4.70 (m, 2 H), 4.88–5.24 (m, 7 H), 7.86–8.20 (m, 3 H). ESI-MS  $m/z$  2085.98  $[M + Na]^+$ . The  $^1H$  NMR spectrum of **8b** was measured after  $Na_2S_2O_4$  in situ reduction of the sample containing the rotaxane **8a**.  $\delta_H$  1.08–1.38 (m, 12 H), 1.40–1.48 (m, 24 H), 1.50–1.65 (m, 4 H), 1.80–1.92 (m, 4 H), 1.95–2.03 (m, 2 H), 2.20–2.28 (m, 5 H), 2.93–2.99 (m, 1 H), 3.30–3.34 (m, 1 H), 3.50–4.20 (m, 46 H), 4.40–4.53 (m, 7 H), 4.60–4.78 (m, 4 H), 4.98–5.21 (m, 9 H), 7.86–8.15 (m, 3 H).  $\delta_C$  23.9, 27.5, 32.2, 32.7, 33.5, 33.9, 38.9, 42.3, 42.8, 42.9, 45.5, 53.3, 53.9, 60.3, 61.9, 62.3, 62.8, 63.0, 63.4, 63.8, 71.3, 72.6, 73.5, 74.2, 74.4, 74.7, 74.9, 75.2, 75.8, 76.1, 76.5, 78.1, 79.5, 83.4, 83.9, 84.0, 85.7, 89.6, 104.2, 104.3, 104.7, 105.6, 127.2, 129.4, 146.7, 147.4, 177.7, 177.9.

## ■ ASSOCIATED CONTENT

### ■ Supporting Information

$^1H$  NMR, 2D-ROESY, ESR spectra, PELDOR decay of **8a**, MD calculations details, atom coordinates for the optimized geometries of carbonyl analogues of **8a**, **9a**, and **10**. This material is available free of charge via the Internet at <http://pubs.acs.org>.

## ■ AUTHOR INFORMATION

### Corresponding Author

marco.lucarini@unibo.it

### Notes

The authors declare no competing financial interest.

## ■ ACKNOWLEDGMENTS

This work was supported by MIUR (Contract 2008KRBLP5) and Alma Mater Studiorum. University of Bologna, Italy.

## ■ REFERENCES

- (1) (a) Ogino, H. *J. Am. Chem. Soc.* **1981**, *103*, 1303–1304. (b) Manka, J. S.; Lawrence, D. S. *J. Am. Chem. Soc.* **1990**, *112*, 2440–2442. (c) Rao, T. V.; Lawrence, D. S. *J. Am. Chem. Soc.* **1990**, *112*, 3614–3615. (d) Wylie, R. S.; Macartney, D. H. *J. Am. Chem. Soc.* **1992**, *114*, 3136–3138. (e) Harada, A.; Li, J.; Kamachi, M. *Chem. Commun.* **1997**, 1413–1414. (f) Anderson, S.; Claridge, T. D. W.; Anderson, H. L. *Angew. Chem., Int. Ed. Engl.* **1997**, *36*, 1310–1313. (g) Murakami, H.; Kawabuchi, A.; Kotoo, K.; Kunitake, M.; Nakashima, N. *J. Am. Chem. Soc.* **1997**, *119*, 7605–7606. (h) Nepogodiev, S. A.; Stoddart, J. F. *Chem. Rev.* **1998**, *98*, 1959–1976. (i) Raymo, F. M.; Stoddart, J. F. *Chem. Rev.* **1999**, *99*, 1643–1664.
- (2) (a) Kawaguchi, Y.; Harada, A. *J. Am. Chem. Soc.* **2000**, *122*, 3797–3798. (b) Onagi, H.; Easton, C. J.; Lincoln, S. F. *Org. Lett.* **2001**, *3*, 1041–1044. (c) Harada, A. *Acc. Chem. Res.* **2001**, *34*, 456–464. (d) Stanier, C. A.; Alderman, S. J.; Claridge, T. D. W.; Anderson, H. L. *Angew. Chem., Int. Ed.* **2002**, *41*, 1769–1772. (e) Onigi, H.; Carrozzini, B.; Cascarano, G. L.; Easton, C. J.; Edwards, A. J.; Lincoln, S. F.; Rae, A. D. *Chem.—Eur. J.* **2003**, *9*, 5971–5977. (f) Wang, Q. C.; Qu, D. H.; Ren, J.; Chen, K.; Tian, H. *Angew. Chem., Int. Ed.* **2004**, *43*, 2661–2665. (g) Easton, C. J.; Lincoln, S. F.; Barr, L.; Onagi, H. *Chem.—Eur. J.* **2004**, *10*, 3120–3128. (h) Nelson, A.; Belitsky, J. M.; Vidal, S.;

- Joiner, C. S.; Baum, L. G.; Stoddart, J. F. *J. Am. Chem. Soc.* **2004**, *126*, 11914–11922. (i) Nijhuis, C. A.; Huskens, J.; Reinhoudt, D. N. *J. Am. Chem. Soc.* **2004**, *126*, 12266–12267. (j) Oshikiri, T.; Takashima, Y.; Yamaguchi, H.; Harada, A. *J. Am. Chem. Soc.* **2005**, *127*, 12186–12187. (k) Liu, Y.; Wang, H.; Chen, Y.; Ke, C. F.; Liu, M. *J. Am. Chem. Soc.* **2005**, *127*, 657–666. (l) Murakami, H.; Kawabuchi, A.; Matsumoto, R.; Ido, T.; Nakashima, N. *J. Am. Chem. Soc.* **2005**, *127*, 15891–15899. (m) Wenz, G.; Han, B.-H.; Muller, A. *Chem. Rev.* **2006**, *106*, 782–817. (n) Liu, Y.; Chen, Y. *Acc. Chem. Res.* **2006**, *39*, 681–691. (o) Park, J. S.; Wilson, J. N.; Hardcastle, K. I.; Bunz, U. H. F.; Srinivasarao, M. *J. Am. Chem. Soc.* **2006**, *128*, 7714–7715. (p) Klotz, E. J. F.; Claridge, T. D. W.; Anderson, H. L. *J. Am. Chem. Soc.* **2006**, *128*, 15374–15375. (q) Cheetham, A. G.; Hutchings, M. G.; Claridge, T. D. W.; Anderson, H. L. *Angew. Chem., Int. Ed.* **2006**, *45*, 1596–1599. (r) Wang, Q. C.; Ma, X.; Qu, D. H.; Tian, H. *Chem.—Eur. J.* **2006**, *12*, 1088–1096. (s) Ma, X.; Wang, Q. C.; Qu, D. H.; Xu, Y.; Ji, F.; Tian, H. *Adv. Funct. Mater.* **2007**, *17*, 829–837. (t) Frampton, M. J.; Anderson, H. L. *Angew. Chem., Int. Ed.* **2007**, *46*, 1028–1064.
- (3) Isnin, R.; Kaifer, A. E. *J. Am. Chem. Soc.* **1991**, *113*, 8188–8190.
  - (4) Buston, J. E. H.; Marken, F.; Anderson, H. L. *Chem. Commun.* **2001**, 1046–1047.
  - (5) (a) Park, J. W.; Song, H. J. *Org. Lett.* **2004**, *6*, 4869–4872. (b) Park, J. W.; Song, H. J.; Chang, H. J. *Tetrahedron Lett.* **2006**, *47*, 3831–3834.
  - (6) Zhao, Y. L.; Dichtel, W. R.; Trabolsi, A.; Saha, S.; Aprahamian, I.; Stoddart, J. F. *J. Am. Chem. Soc.* **2008**, *130*, 11294–11296.
  - (7) Craig, M. R.; Hutchings, M. G.; Claridge, T. D. W.; Anderson, H. L. *Angew. Chem., Int. Ed.* **2001**, *40*, 1071–1074.
  - (8) (a) Wang, Q. C.; Qu, D. H.; Ren, J.; Chen, K.; Tian, H. *Angew. Chem., Int. Ed.* **2004**, *43*, 2661–2665. (b) Qu, D. H.; Wang, Q. C.; Ren, J.; Tian, H. *Org. Lett.* **2004**, *6*, 2085–2088. (c) Wang, Q. C.; Ma, X.; Qu, D. H.; Tian, H. *Chem.—Eur. J.* **2006**, *12*, 1088–1096. (d) Tomatsu, I.; Hashidzume, A.; Harada, A. *Angew. Chem., Int. Ed.* **2006**, *45*, 4605–4608. (e) Oshikiri, T.; Takashima, Y.; Yamaguchi, H.; Harada, A. *Chem.—Eur. J.* **2007**, *13*, 7091–7098.
  - (9) Chwalek, M.; Auzély, R.; Fort, S. *Org. Biomol. Chem.* **2009**, *7*, 1680–1688.
  - (10) Steinhoff, H. J. *Front. Biosci.* **2002**, *7*, 97–110.
  - (11) Eaton, S. S.; Eaton, G. R. In *Biological Magnetic Resonance*; Berliner, L. J., Eaton, S. S., Eaton, G. R., Eds.; Kluwer Academic/Plenum Publishers: New York, 2000; Vol 19, pp 2–28.
  - (12) Tsvetkov, Yu. D. In *Biological Magnetic Resonance*; Berliner, L. J., Bender, C. J., Eds.; Kluwer Academic/Plenum Publishers: New York, 2004; Vol. 21, pp 385–433.
  - (13) Jeske, G.; Pannier, M.; Spiess, H. W. In *Biological Magnetic Resonance*; Berliner, L. J., Eaton, S. S., Eaton, G. R., Eds.; Kluwer Academic/Plenum Publishers: New York, 2000; Vol. 19, pp 493–512.
  - (14) Borbat, P. P.; Freed, J. F. In *Biological Magnetic Resonance*; Berliner, L. J., Eaton, S. S., Eaton, G. R., Eds.; Kluwer Academic/Plenum Publishers: New York, 2000; Vol. 19, pp 383–460.
  - (15) Krock, L.; Shivanyuk, A.; Goodin, D. B.; Rebek, J. *Chem. Commun.* **2004**, 272–273.
  - (16) (a) Araki, K.; Nakamura, R.; Otsuka, H.; Shinkai, S. *J. Chem. Soc., Chem. Commun.* **1995**, 2121–2122. (b) Rajca, A.; Mukherjee, S.; Pink, M.; Rajca, S. *J. Am. Chem. Soc.* **2006**, *128*, 13497–13507.
  - (17) Chechik, V.; Ionita, G. *New J. Chem.* **2007**, *31*, 1726–1729.
  - (18) Mezzina, E.; Fani, M.; Ferroni, F.; Franchi, P.; Menna, M.; Lucarini, M. *J. Org. Chem.* **2006**, *71*, 3773–3777.
  - (19) (a) Mileo, E.; Casati, C.; Franchi, P.; Mezzina, E.; Lucarini, M. *Org. Biomol. Chem.* **2011**, *9*, 2920–2924. (b) Mezzina, E.; Cruciani, F.; Pedulli, G. F.; Lucarini, M. *Chem.—Eur. J.* **2007**, *13*, 7223–7233.
  - (20) Pievo, R.; Casati, C.; Franchi, P.; Mezzina, E.; Bennati, M.; Lucarini, M. *ChemPhysChem* **2012**, *13*, 2659–2661.
  - (21) (a) Zhao, N.; Lloyd, G. O.; Scherman, O. A. *Chem. Commun.* **2012**, *48*, 3070–3072. (b) Lucas, D.; Minami, T.; Iannuzzi, G.; Cao, L.; Wittenberg, J. B.; Anzenbacher, P.; Isaacs, L. *J. Am. Chem. Soc.* **2011**, *133*, 17966–17976.
  - (22) Bellia, F.; La Mendola, D.; Pedone, C.; Rizzarelli, E.; Saviano, M.; Vecchio, G. *Chem. Soc. Rev.* **2009**, *38*, 2756–2781.

- (23) (a) Paton, R. M.; Kaiser, E. T. *J. Am. Chem. Soc.* **1970**, *92*, 4723–4725. (b) Ionita, G.; Chechik, V. *Org. Biomol. Chem.* **2005**, *3*, 3096–3098. (c) Bardelang, D.; Rockenbauer, A.; Jicsinszky, L.; Finet, J.-P.; Karoui, H.; Lambert, S.; Marque, S. R. A.; Tordo, P. *J. Org. Chem.* **2006**, *71*, 7657–7667. (d) Bardelang, D.; Finet, J.-P.; Jicsinszky, L.; Karoui, H.; Marque, S. R. A.; Rockenbauer, A.; Rosas, R.; Charles, L.; Monnier, V.; Tordo, P. *Chem.—Eur. J.* **2007**, *13*, 9344–9354.
- (24) Franchi, P.; Fani, M.; Mezzina, E.; Lucarini, M. *Org. Lett.* **2008**, *10*, 1901–1904.
- (25) (a) Melton, L. D.; Slessor, K. N. *Carbohydr. Res.* **1971**, *18*, 29–37. (b) Teranishi, K.; Watanabe, K.; Hisamatsu, M.; Yamada, T. *J. Carbohydr. Chem.* **1998**, *17*, 489–494.
- (26) Luo, J.; Pardin, C.; Lubell, W. D.; Zhu, X. X. *Chem. Commun.* **2007**, 2136–2138.
- (27) Martina, K.; Trotta, F.; Robaldo, B.; Belliardi, N.; Jicsinszky, L.; Cravotto, G. *Tetrahedr. Lett.* **2007**, *48*, 9185–9189. The reported procedure for the preparation of the azido derivative was slightly modified as follows. Sodium azide (0.39 g, 6.0 mmol) was added to a solution of mono-2-*O-p*-tosyl- $\alpha$ -CD (0.75 g, 0.61 mmol) in DMF (10 mL). The solution was stirred at 100 °C overnight and evaporated under reduced pressure. The crude residue was purified by column chromatography (CH<sub>3</sub>CN/H<sub>2</sub>O, 8:2), affording the product (0.46 g, 75%).  $\delta_{\text{H}}$  (300 MHz, DMSO-*d*<sub>6</sub>) 3.25–3.35 (m, 12 H), 3.45–4.00 (m, 18 H), 4.40–4.55 (m, 6 H), 4.79 (bs, 6 H), 5.40–5.70 (m, 11 H). MS-ESI: *m/z* = 1020 [M + Na]<sup>+</sup>.
- (28) It is known that nucleophilic substitution of 2-(*p*-toluenesulfonyl) $\alpha$ CD afforded a monosubstituted cyclodextrin substituted at the 3 position. For a thorough discussion see ref 27.
- (29) (a) Spevak, W.; Dasgupta, F.; Hobbs, C. J.; Nagy, J. O. *J. Org. Chem.* **1996**, *61*, 3417–3422. (b) Lockhoff, O. *Angew. Chem., Int. Ed. Engl.* **1991**, *30*, 1611–1620. (c) Larpent, C.; Laplace, A.; Zemb, T. *Angew. Chem., Int. Ed.* **2004**, *43*, 3163–3167.
- (30) According to NMR results, only one radical species was observed indicating the presence of only one isomer. As already observed with the rotaxane mixture **6a–7a**, the possible presence of another isomer could not be detected because the spectral parameters are not sufficiently different.
- (31) (a) Müick, S. M.; Martinez, G. V.; Fiori, W. R.; Todd, A. P.; Millhauser, G. L. *Nature* **1992**, *359*, 653–655. (b) Fiori, W. R.; Lundberg, K. M.; Millhauser, G. L. *Nat. Struct. Biol.* **1994**, *1*, 374–377. (c) Fiori, W. F.; Müick, S. M.; Millhauser, G. L. *Biochemistry* **1993**, *32*, 11957–11962.
- (32) Hanson, P.; Millhauser, G.; Formaggio, F.; Crisma, M.; Toniolo, C. *J. Am. Chem. Soc.* **1996**, *118*, 7618–7625.
- (33) Carlotto, S.; Cimino, P.; Zerbetto, M.; Franco, L.; Corvaja, C.; Crisma, M.; Formaggio, F.; Toniolo, C.; Polimeno, A.; Barone, V. *J. Am. Chem. Soc.* **2007**, *129*, 11248–11258.
- (34) Ionita, G.; Meltzer, V.; Pincuc, E.; Chechik, V. *Org. Biomol. Chem.* **2007**, *5*, 1910–1914.
- (35) Yi, S.; Captain, B.; Ottaviani, M. F.; Kaifer, A. E. *Langmuir* **2011**, *27*, 5624–5632.
- (36) Nakabayashi, K.; Kawano, M.; Yoshizawa, M.; Ohkoshi, S.; Fujita, M. *J. Am. Chem. Soc.* **2004**, *126*, 16694–16695.
- (37) Luckhurst, G. R. *Mol. Phys.* **1966**, *30*, 543–550.
- (38) Parmon, V. N.; Kokorin, A. I.; Zhidomirov, G. M.; Zamarev, K. I. *Mol. Phys.* **1975**, *30*, 695–701.
- (39)  $I_2/I_1 \approx d_2(\Delta H_2)^2/d_1(\Delta H_1)^2$  where  $d_1$  and  $d_2$  are the line amplitudes and  $\Delta H_2$  and  $\Delta H_1$  are the corresponding widths.
- (40) Szydłowska, J.; Pietrasik, K.; Glaz, L.; Kaim, A. *Chem. Phys. Lett.* **2008**, *460*, 245–252.
- (41) Lucarini, M.; Luppi, B.; Pedulli, G. F.; Roberts, B. P. *Chem.—Eur. J.* **1999**, *5*, 2048–2054.
- (42) Yu, Y.; Cai, W.; Chipot, C.; Sun, T.; Shao, X. *J. Phys. Chem. B* **2008**, *112*, 5268–5271.
- (43) Franchi, P.; Lucarini, M.; Mezzina, E.; Pedulli, G. F. *J. Am. Chem. Soc.* **2004**, *126*, 4343–4354.
- (44) Milov, A. D.; Salikhov, K. M.; Shirov, M. D. *Fiz. Tverd. Tela* **1981**, *23*, 975–982.
- (45) Milov, A. D.; Ponomarev, A. B.; Tsvetkov, Y. D. *Chem. Phys. Lett.* **1984**, *110*, 67–72.
- (46) Martin, R. E.; Pannier, M.; Diederich, F.; Gramlich, V.; Hubrich, M.; Spiess, H. W. *Angew. Chem., Int. Ed.* **1998**, *37*, 2833–2837.
- (47) Jeschke, G.; Koch, A.; Jonas, U.; Godt, A. *J. Magn. Reson.* **2002**, *155*, 72–82.
- (48) (a) Yamaguchi, K.; Okumura, M.; Maki, J.; Noro, T.; Namimoto, H.; Nakano, M.; Fueno, T.; Nakasuji, K. *Chem. Phys. Lett.* **1992**, *190*, 353–360. (b) Closs, G. L.; Forbes, M. D. E.; Piotrowiak, P. *J. Am. Chem. Soc.* **1992**, *114*, 3285–3294.
- (49) Barone, V.; Bencini, A.; Di Matteo, A. *J. Am. Chem. Soc.* **1997**, *119*, 10831–10837.
- (50) Fritscher, J.; Beyer, M.; Schiemann, O. *Chem. Phys. Lett.* **2002**, *364*, 393–401.
- (51) Another important example supporting this view is given by the octapeptide reported by Sartori et al.,<sup>52</sup> characterized by three nitroxides residues. The octapeptide forms in acetonitrile a rigid  $3_{10}$ -helix structure in which they are placed in a linear configuration one on top of the other after one helix turn. The distance between the midpoints of the farthest N–O bonds is 12 Å, and the corresponding exchange constant, *J* is close to 0.
- (52) Sartori, E.; Corvaja, C.; Oancea, S.; Formaggio, F.; Crisma, M.; Toniolo, C. *ChemPhysChem* **2005**, *6*, 1472–1475.